Chemical Science

ROYAL SOCIETY OF CHEMISTRY

MINIREVIEW

View Article Online
View Journal | View Issue

Cite this: *Chem. Sci.*, 2020, **11**, 4297

All publication charges for this article have been paid for by the Royal Society of Chemistry

Received 7th February 2020
Accepted 5th April 2020

DOI: 10.1039/d0sc00735h

rsc.li/chemical-science

Solid-state NMR spectroscopy: an advancing tool to analyse the structure and properties of metal–organic frameworks

Eike Brunner * and Marcus Rauche

Metal–organic frameworks (MOFs) gain increasing interest due to their outstanding properties like extremely high porosity, structural variability, and various possibilities for functionalization. Their overall structure is usually determined by diffraction techniques. However, diffraction is often not sensitive for subtle local structural changes and ordering effects as well as dynamics and flexibility effects. Solid-state nuclear magnetic resonance (ssNMR) spectroscopy is sensitive for short range interactions and thus complementary to diffraction techniques. Novel methodical advances make ssNMR experiments increasingly suitable to tackle the above mentioned problems and challenges. NMR spectroscopy also allows study of host–guest interactions between the MOF lattice and adsorbed guest species. Understanding the underlying mechanisms and interactions is particularly important with respect to applications such as gas and liquid separation processes, gas storage, and others. Special *in situ* NMR experiments allow investigation of properties and functions of MOFs under controlled and application-relevant conditions. The present minireview explains the potential of various solid-state and *in situ* NMR techniques and illustrates their application to MOFs by highlighting selected examples from recent literature.

Metal–organic frameworks: general aspects and recent analytical challenges

Metal–organic frameworks (MOFs)[1–5] are built from inorganic secondary building units (SBUs) and organic ligands (*cf.* Fig. 1).

Chair of Bioanalytical Chemistry, Faculty of Chemistry and Food Chemistry, TU Dresden, 01062 Dresden, Germany. E-mail: eike.brunner@tu-dresden.de

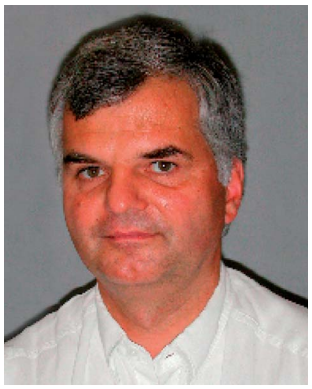

Eike Brunner received a diploma in physics (1987) and a Ph.D. (1989) from the University of Leipzig. Following a post-doctoral research stay at the Fritz Haber Institute of the Max Planck Society in 1990/1991, he was habilitated in 1996 (University of Leipzig) and received a Heisenberg fellowship from the DFG. After a research stay at the University of California at Berkeley in 1997/1998, he became Professor of Biophysics at the University of Regensburg (2001). Since 2007, he has been Professor for Bioanalytical Chemistry at TU Dresden. His research focuses on the NMR spectroscopic investigation of materials such as biominerals and MOFs.

Marcus Rauche studied chemistry and received his Bachelor's (2013) and Master's (2015) degrees from TU Dresden. In 2016, he started working on his PhD thesis at TU Dresden dealing with the NMR spectroscopic characterisation of flexible MOFs.

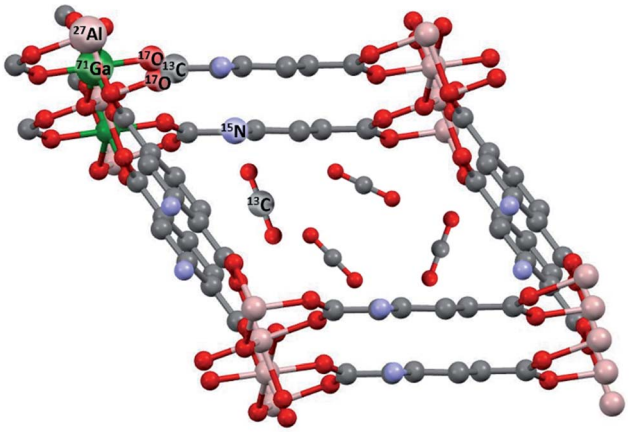

Fig. 1 Typical NMR-active nuclei found in MOFs like MIL-53 (ref. 6) and their modifications. NH_2-functionalized linkers are depicted as used in MIL-53-NH_2(as).[7] This topology was also prepared as a mixed-metal compound MIL-53(Al/Ga),[8] see below. *In situ* NMR can detect adsorbed molecules like $^{13}CO_2$ and their interactions with the MOF.

These components are linked together by coordination bonds thus forming highly porous and functional crystalline solids with specific surface areas up to 7800 $m^2\ g^{-1}$.[5] Various novel MOFs have been synthesized employing a multitude of different SBUs and linkers during the last few years.[4] MOFs stand out due to their extremely high porosity compared with other porous materials. Linker functionalization offers the possibility to introduce special functionalities into the structure and to vary the pore size/geometry in a controlled fashion. For these reasons, MOFs are intensively studied as one of the most promising platforms for gas storage, separation, and purification and also for catalysis.

The crystal structure of MOFs is commonly determined by diffraction techniques. However, MOF lattices exhibit various important properties which cannot or only partly be addressed by diffraction methods. The following challenges for MOF characterization can for example be tackled by NMR:

Local structure and order

As an example, MOFs with mixed metal sites or mixed linkers often pose problems because the distribution of the different metals or linkers in the framework is hardly accessible for diffraction methods. Incorporation and distribution of functionalities like linker side chains or nanoparticle catalysts in MOF crystallites is another example.

Local and global flexibility

MOF lattices can exhibit different types of flexibility which can be subdivided into local and global effects. Globally "rigid" MOF structures can exhibit local motions, *e.g.*, of the linkers, linker side chains, or functional groups. Such motions can be important for properties like adsorption behaviour. Furthermore, guest adsorption can result in subtle local structural changes even in "rigid" MOFs. A small subgroup of MOFs exhibits very pronounced global porosity switching in the crystalline solid state. These compounds are denoted as flexible, switchable, or "3rd generation" MOFs.[3] Selected examples are MIL-53 (MIL: Materials of Institute Lavoisier[6]) and DUT-8 (DUT: Dresden University of Technology[9]). DUT-8 exhibits an adsorption-induced gating transition accompanied by a tremendous unit cell volume change of more than 100%! The mechanisms underlying these pronounced transitions are still insufficiently understood and need further investigation.

Host–guest interactions and functional behaviour

In situ techniques[10] are important for the investigation of MOFs under conditions relevant for later applications like adsorption and storage, separation, and catalysis, or for use as sensors. Such studies often require special experimental setups for *in situ* experiments on MOFs, for example under controlled loading, external gas pressure, educt flow in catalytic reactions, external electric fields, or mechanical pressure.

Principles of solid-state NMR spectroscopy

Solid-state nuclear magnetic resonance (ssNMR) spectroscopy provides short-range, *i.e.*, local structural information and is sensitive for local dynamics/thermal motions.

Short-range internal interactions

NMR in condensed matter was reported for the first time in 1946 (ref. 11 and 12) (Nobel prize 1952). In 1948, Pake[13] described the very broad and characteristic ^{1}H NMR line shape of crystal water molecules in gypsum, which is now called the Pake doublet. It is dominated by the homo-nuclear magnetic dipole–dipole interaction (dipole coupling) between the two neighbouring ^{1}H spins in crystal water. In this special case, straightforward line shape analysis allows inter-nuclear distance determination. Heteronuclear dipole coupling between different nuclear spins (*e.g.*, ^{13}C and ^{15}N) is another distance-dependent interaction. This means dipole coupling makes distance information accessible for ssNMR experiments without the need of long-range order in contrast to diffraction-based crystallography. Further important interactions are the chemical shift anisotropy (CSA), the electric quadrupole interaction for nuclei with spin quantum numbers $I > \frac{1}{2}$, or electron–nucleus interactions, *i.e.*, hyperfine couplings in compounds with paramagnetic sites (see below).[14–16] CSA reflects the spatial anisotropy of the chemical shift in solids (*cf.* Fig. 4 and related text below). The electric quadrupole interaction depends on the electric field gradient tensor at the site of the detected nucleus and dominates, *e.g.*, the ^{2}H NMR line shape in deuterated solids (*cf.* Fig. 3). These favourable properties verify ssNMR spectroscopy to be an excellent tool for structural analyses of solids.[14–16]

High-resolution ssNMR spectroscopy

Typically, the simultaneous presence of various line-broadening interactions of comparable strength leads to broad but featureless Gaussian lines in solids. The invention of the magic

angle spinning (MAS) technique[17] was a major breakthrough for ssNMR spectroscopy. It relies on rapid sample spinning around an axis tilted against the external magnetic field B_0 by the "magic angle" of 54.74°. This averages anisotropic interactions in analogy to the influence of isotropic molecular re-orientation in liquids and allows resolution of lines with different chemical shifts in solids. Continuous methodical development over decades now allows ultrafast MAS experiments at rates beyond 120 kHz.[18] Ultrafast spinning is particularly important for systems with strong homo-nuclear dipole couplings between more than two spins[19] like ^{1}H-rich solids.[20] Combination of MAS with cross-polarization (CP)[21] enables sensitive detection of well-resolved CP MAS NMR spectra[22] of intrinsically insensitive nuclei like ^{13}C, ^{15}N, or others. Cross-polarization is often used in two-dimensional (2D) hetero-nuclear correlation (HETCOR) spectroscopy. Application of MAS, however, removes anisotropic interactions like the dipole couplings which bear the distance information. Special experiments allow selective re-introduction of desired interactions under MAS. An example is rotational echo double resonance (REDOR).[23] It allows measurement of inter-nuclear distances in hetero-nuclear spin pairs like ^{13}C–^{15}N.

Solid-state NMR spectroscopy of MOFs

Solid-state NMR spectroscopy is increasingly applied to MOFs[24–26] based on the detection of NMR-active nuclei in their framework (*cf.* Fig. 1). Detection of metal ions is possible for SBUs containing NMR-active nuclei. Examples are ^{27}Al or ^{51}V which exhibit high natural abundance and a moderately high magnetic moment.[27] Various commonly used metal ions in MOFs exhibit NMR-active isotopes with low natural abundance and small magnetic moments, for example ^{25}Mg and ^{67}Zn.[28–30] Special pulse sequences like CPMG (Carr–Purcell–Meiboom–Gill) can enhance the NMR signal thus enabling detection of such spectra. In addition, quadrupolar nuclei often exhibit very broad lines. Broad-band pulses or sequences like WURST (wideband uniform rate smooth truncation) must then be used to excite a sufficiently large frequency range.[31]

Direct ssNMR detection of the nuclei in paramagnetic ions like Cr, Mn, Fe, Co, Ni, or Cu is often difficult or impossible. But it is sometimes feasible to study signals of nuclei close to the SBU. Examples are ^{13}C or ^{17}O in coordinating carboxylates of the linker molecules. These neighbouring nuclei act as "reporters" *via* their interactions with the paramagnetic centres in the SBU. It is possible to exploit characteristic effects like the Fermi contact and pseudo-contact shifts caused by paramagnetic centres, which are observable in the NMR signals of neighbouring nuclear spins.[16] This is also true for SBUs with di-metal sites, *e.g.*, typical paddle wheel units with antiferromagnetic coupling in their ground state[32] because excited states may nevertheless be paramagnetic and can influence the NMR signals.[33] In any case, the NMR signals of nuclei in the SBUs as well as neighbouring nuclei in the linkers like ^{1}H/^{2}H, ^{13}C, or ^{15}N contain valuable information as illustrated for selected examples in the following.

Local structure and order

Benzaqui *et al.*[34] visualized subtle structural differences in the Al environment between hydrated and dehydrated MIL-96(Al) which were not found by X-ray diffraction. ^{27}Al MAS NMR and 2D double-quantum–single-quantum (DQ–SQ) MAS NMR spectroscopy were applied. As can be seen in Fig. 2, dehydration of the sample results in a structural change of the Al3 site as reflected by a splitting into two signals denoted by Al3 and Al3′. Density functional theory (DFT) calculations provided a structural model for the responsible interactions between water molecules and the SBUs. The calculations agree well with the measured ^{27}Al chemical shifts and quadrupole coupling constants. These observations emphasize the high sensitivity of ssNMR spectroscopy for subtle local structural changes in SBUs and highlight the usefulness of DFT combined with ssNMR spectroscopy.

Mali *et al.*[35] studied the ion distribution in the metal oxo trimers of mixed-metal MIL-100(Fe/Al) by combining ^{27}Al MAS NMR, EPR (electron paramagnetic resonance) and Mössbauer

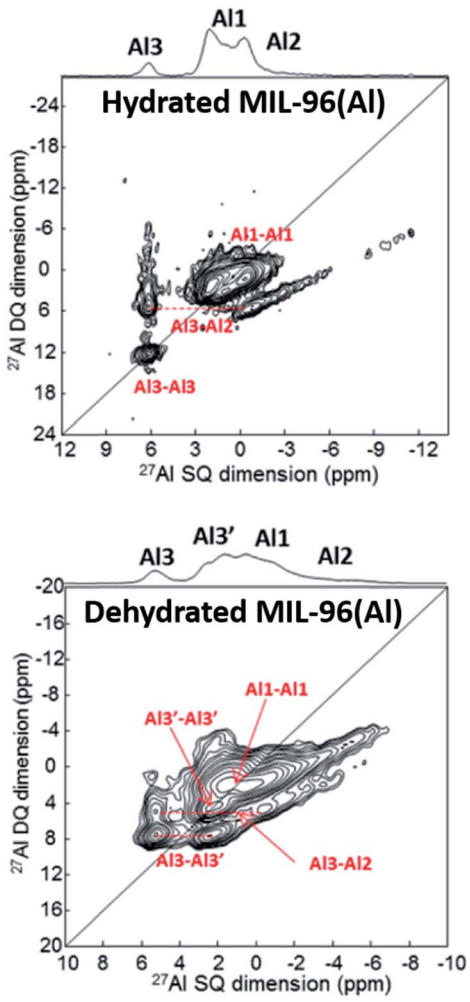

Fig. 2 ^{27}Al DQ–SQ spectra of MIL-96(Al) showing the influence of the hydration state upon the environment of Al. Adapted with permission.[34] Copyright 2017, American Chemical Society.

spectroscopy as well as EXAFS (extended X-ray absorption fine structure) and DFT. Paramagnetic shifts of ^{27}Al occurred due to hyperfine interactions with the paramagnetic Fe species. These shifts are proportional to the hyperfine coupling constant and could be well reproduced by first-principles calculations. Random distribution of Al and Fe in the metal oxo trimers of MIL-100(Fe/Al) could be inferred from this study.

Oxygen, *e.g.*, in carboxylate-based linkers, is located next to the metal centres and is sensitive to changes in the SBU. ^{17}O NMR spectroscopy usually requires isotope enrichment because the natural abundance of this isotope only amounts to 0.05%. Bignami *et al.*[8] described a cost-effective route to ^{17}O-enriched terephthalic acid linkers in mixed-metal MIL-53(Al/Ga) by the so-called dry gel conversion (DGC) method. A pre-dried gel containing linker molecules and metal salt is treated in an autoclave with vapor generated by a small amount of water at elevated temperature. The cation distribution in this mixed metal MOF could be studied by ^{17}O multiple-quantum (MQ) MAS and DOR (double rotation) NMR spectroscopy. The presence of Al and Ga bridged by one hydroxyl species was observed. It is thus concluded that the two metals do not separate and MIL-53(Al/Ga) is a true mixed-metal material. The discussed publications nicely demonstrate that ssNMR spectroscopy can elucidate the metal ion distribution in mixed-metal MOFs.

The linker distribution in MOFs with mixed linkers was studied by the Reimer group[36] using the REDOR technique. The two linkers exhibit different functional groups selectively labelled with either ^{13}C or ^{15}N. The ^{13}C–^{15}N REDOR experiments performed allowed measurement of the average distance between the ^{13}C and ^{15}N nuclei located in the two different linkers. Based on molecular dynamics (MD) simulations, it became possible to derive a linker distribution model consistent with the measured distance.

Local thermal motions

Zhu *et al.*[37] described the incorporation of a so-called "molecular shuttle" performing translational motions into a MOF denoted as UWDM-4 (UWDM: University of Windsor Dynamic Material). The motions of this molecular shuttle within the framework were demonstrated by ^{13}C CP MAS NMR and 2D exchange spectroscopy (EXSY, see below).

Linker molecules or certain parts of them like phenyl rings and attached side groups often exhibit thermal motions such as rotations and vibrations. ^{2}H NMR spectroscopy is a powerful method to visualize and study such local motions.[38] In favourable cases, not only can the specific motional mode of the linker be deduced, but it may also be possible to measure the motional frequency/exchange rate by line shape analysis of the ^{2}H NMR signal.[38] For example, Khudozhitkov *et al.*[39] investigated 180° phenyl ring flips about the C2 axis of the linkers in $[M_2(bdc)_2(dabco)]$ (M = Zn, Ni, Co, Cu; bdc = 1,4-benzene dicarboxylate, terephthalate; dabco = 1,4 diazabicyclo[2.2.2]octane). As indicated in Fig. 3 (right), the phenyl ring flip rate k slows down from 6000 kHz to 20 kHz after loading the MOF with dimethylformamide (DMF). For slow flips (20 kHz), the line shape almost perfectly corresponds to a Pake doublet with *ca.* 120 kHz frequency distance between the two intensity maxima. This is characteristic for rigid ^{2}H–C groups. The line shape changes significantly for fast 180° flips (6000 kHz) present in the DMF-free sample. Line shape analysis allows determination of the exchange rate quantitatively.

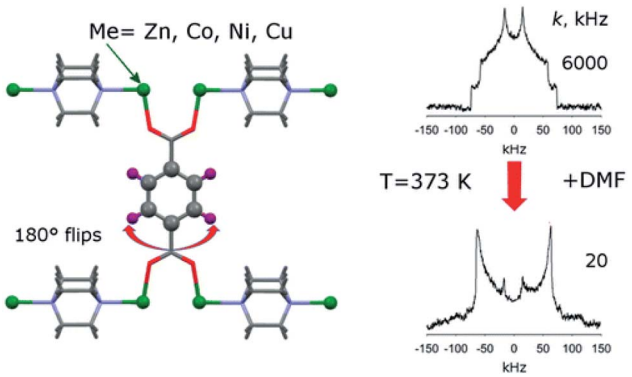

Fig. 3 Illustration of typical ^{2}H NMR line shapes and the influence of 180° flips of linker phenyl groups. Reproduced[39] with permission. Copyright 2015, American Chemical Society.

In situ NMR and host–guest interaction studies

Experiments under MAS

MAS NMR studies of host–guest interactions are usually performed on sealed samples loaded with liquids or gases. They sometimes require high pressures and/or temperatures. Standard MAS NMR probes operate at temperatures between *ca.* 120 and 370 K. Common MAS rotors do not allow high pressures because the rotor caps are not pressure tight. Therefore, increasing efforts are made to construct special *in situ* MAS probes and rotors. A sealed MAS NMR rotor system allowing temperatures and pressures up to 520 K and 100 bar was developed by Hu *et al.*[40] Even higher temperatures at lower pressures are feasible, *e.g.*, using high-frequency (hf)-heated rotor inserts.[41] The synthesis of various materials including MOFs can be monitored by *in situ* liquid-state and solid-state NMR spectroscopy as reviewed by Haouas.[42] An elegant combination of liquid- and solid-state NMR spectroscopy is denoted as CLASSIC (combined liquid- and solid-state *in situ* crystallization). It is performed on identical samples under MAS by interleaved detection of directly excited and cross-polarization spectra.[43]

Gas loaded samples must be kept in tight containers like sealed glass ampoules. Such ampoules can even be inserted into MAS rotors if manufactured properly.[44] Experiments are then performed at constant loading with a defined number of molecules or atoms before sample sealing. Temperature variation causes pressure changes because the adsorption equilibrium is temperature-dependent. However, exact pressure determination is then difficult.

Experiments under controlled pressure

It is thus often advantageous to run *in situ* gas adsorption measurements in a fashion where both thermodynamic variables, pressure and temperature, are under external control. Such *in situ* NMR data can directly be correlated with the results of volumetric adsorption experiments. On the other hand, this approach is hardly compatible with MAS because it requires the connection of the sample container with an outside gas reservoir for equilibration after temperature variation. However, *in situ* NMR without MAS can nevertheless deliver valuable information because thermal motions of the adsorbed species often result in sufficiently narrow signals. A corresponding experimental setup was described in ref. 45.

Examples for host–guest interaction studies

Carboxylate ^{13}C nuclei in MOFs with linkers coordinated with the SBUs *via* carboxylate groups are another probe close to the SBU. The natural isotopic abundance of ^{13}C amounts to only 1.1%. Isotope enrichment of carboxylate carbon positions in 2,6-ndc (ndc: naphthalene dicarboxylate) was established and used to study the flexible compound DUT-8(Ni).[46] The labelled carboxylates are then sensitively and selectively detected by ^{13}C CP MAS NMR and a striking influence of solvent polarity upon the chemical shift was observed. This might indicate a specific interaction between the paddle wheel units and polar solvent molecules in contrast to non-polar solvents.

The Senker group functionalized terephthalate linkers in MIL-101(Al) and MIL-101(Cr) by incorporation of 2-pyridyl urea (URPy) side groups resulting in the formation of so-called hydrogen bond donor–donor–acceptor patterns.[47] Their influence upon the sorption selectivity was investigated by competitive adsorption of 2-aminopyridine (2-AP) and 3-aminopyridine (3-AP). ^{15}N ssNMR spectroscopy on ^{15}N-labeled samples was applied to elucidate structural reasons for the significantly higher selectivity coefficients for 3-AP observed on MIL-101-URPy compared with MIL-101-NH_2. This highlights the potential of ssNMR spectroscopy to elucidate the structure of adsorption complexes in MOFs.

Adsorption of CO_2 on MOFs is increasingly studied because CO_2 capture and storage is an environmentally important problem. MOFs are potent materials not only for gas storage but also for separation, *e.g.*, removal of CO_2 from other gases like methane. Various ^{13}C NMR investigations of CO_2 adsorbed on MOFs were reported meanwhile as can be found in the recent review by Witherspoon *et al.*[48] Interaction of CO_2 with open Mg sites in Mg-MOF-74 revealed a line shape characteristic of chemical shift anisotropy but with a reduced width compared to that of rigid CO_2.[49] It was concluded that adsorbed CO_2 jumps between different open metal sites. The resulting partial averaging of the chemical shift anisotropy gives rise to the observed residual chemical shift anisotropy. Similar line shapes are also observed in other MOFs with and without open metal sites.[50–54] Fig. 4 shows the 1D *in situ* ^{13}C NMR and the 2D EXSY spectrum of adsorbed $^{13}CO_2$ in a MOF. Isotropically reorienting free CO_2 gas in the inter-particle space gives rise to a narrow signal at *ca.* 126 ppm. Adsorbed CO_2 shows a characteristic broad signal of

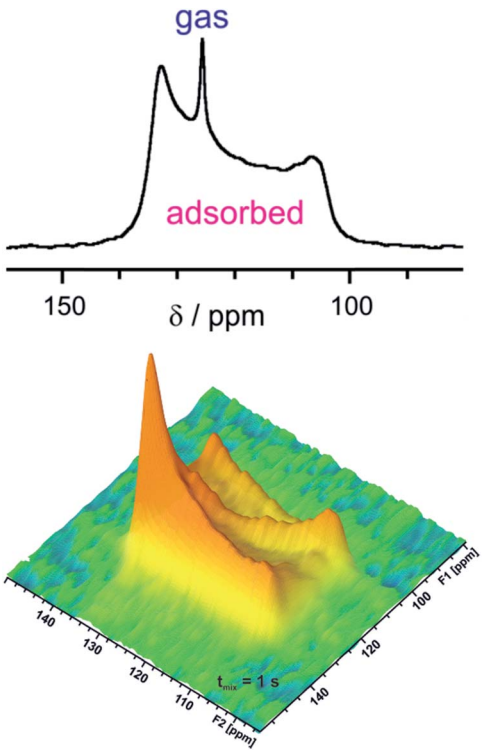

Fig. 4 *In situ* ^{13}C NMR spectrum (5 bar pressure, top) and 2D EXSY spectrum (7 bar pressure, bottom) for CO_2 adsorbed on [Zn_2(bdc)$_2$-dabco] measured at 232 K with 1 s mixing time t_{mix}. Data adapted[50] with permission. Copyright 2015, Elsevier.

ca. 30 ppm overall line width due to the aforementioned residual chemical shift anisotropy. Rigid $^{13}CO_2$ would give a similarly shaped but much broader line of 335 ppm width. The 2D EXSY experiment visualizes slow exchange processes on a large time scale compared with $(2\pi\Delta\nu)^{-1}$ where $\Delta\nu$ is the resonance frequency difference between the involved sites. At short mixing times, only diagonal signals are observed. The strong off-diagonal intensity at 1 s mixing time shows the presence of slow CO_2 exchange between MOF crystallites within t_{mix}. This means the chosen mixing time defines the time scale of exchange.

Adsorption of methane by MOFs is also of great interest because natural gas is a promising carrier for mobile applications. Yan *et al.*[55] used ^2H NMR spectroscopy of samples with deuterated linkers combined with neutron powder diffraction on samples loaded with deuterated methane to investigate methane adsorption in the MOFs MFM-112a, MFM-115a, and MFM-132a (MFM: Manchester Framework Material). It was shown that an optimal combination of linker dynamics, pore geometry, and favorable binding sites is responsible for the favorable methane uptake by these materials.

The selectivity of carbon dioxide adsorption from $^{13}CO_2/^{13}CH_4$ mixtures by flexible MOFs was investigated by *in situ* ^{13}C NMR spectroscopy.[56] This is possible since the characteristic residual chemical shift anisotropy of adsorbed CO_2 and the narrow signal of the gas phase (*cf.* Fig. 4) allow quantitative determination of the ratio between adsorbed and gaseous CO_2.

Adsorbed and gas phase CH_4 molecules can be discriminated by their different isotropic chemical shifts. Microscopic diffusion of pure and mixed methane and carbon dioxide in ZIF-11 (ZIF: zeolitic imidazolate framework) was studied by high field diffusion NMR spectroscopy.[57]

^{129}Xe NMR spectroscopy[58] delivers information on surface chemical properties and the porosity of materials. It is frequently used to characterize host–guest interactions and dynamic phenomena in MOFs. Note that MOFs are also considered for noble gas mixture separations, *e.g.* of Xe/Kr mixtures.

The influence of linker functionalization upon the noble gas adsorption properties of CAU-1 (CAU: Christian Albrecht University, Kiel) could be visualized and studied by *in situ* ^{129}Xe NMR spectroscopy using hyperpolarized ^{129}Xe.[59] The chemical shift sensitively reflects even minor changes in the accessible pore volume caused by functionalisation. This highlights the potential of ^{129}Xe NMR spectroscopy for porosity characterization.

Flexibility studied by *in situ* ^{129}Xe NMR spectroscopy

Hyperpolarized ^{129}Xe NMR spectroscopy was also used to characterize the adsorption-induced structural changes in MIL-53(Al).[60] Further studies on MIL-53(Al) were carried out with and without MAS on sealed samples loaded with defined amounts of xenon.[61] This allowed characterizing the exchange processes between adsorbed xenon in the large-pore form and in the narrow-pore form of the MOF at temperatures where both states co-exist. High-pressure *in situ* ^{129}Xe NMR spectroscopy was used to study adsorption-induced structural changes in flexible MOFs. It was, for example, shown that the gating transition in DUT-8(Ni) is an immediate and complete structural switching process accompanied by complete pore filling at the gate pressure.[45]

Recently, the counterintuitive negative gas adsorption (NGA) phenomenon[62] in DUT-49 and its homologs was studied by *in situ* ^{129}Xe NMR spectroscopy (*cf.* Fig. 5).[63,64] NGA is caused by sudden mesopore contraction at a certain pressure (here: $p/p_0 = 0.18$; p_0 denotes the boiling pressure at the given temperature). Some of the gas adsorbed before in the *open-pore* state is released (NGA) during pore contraction which results in an increased density and intimate contact of xenon with the walls in the *contracted-pore* state. This causes a tremendous chemical shift jump of *ca.* 100 ppm. Re-opening of the pore system at higher relative pressure then gives rise to an increasingly intense signal at a lower chemical shift (Fig. 5).

Finally, MOFs are also considered for catalysis and electrode applications. *In situ* NMR spectroscopic approaches for monitoring catalytic reactions[65] and electro-adsorption in electrochemical devices under operating conditions[66] already exist and are used for other materials.

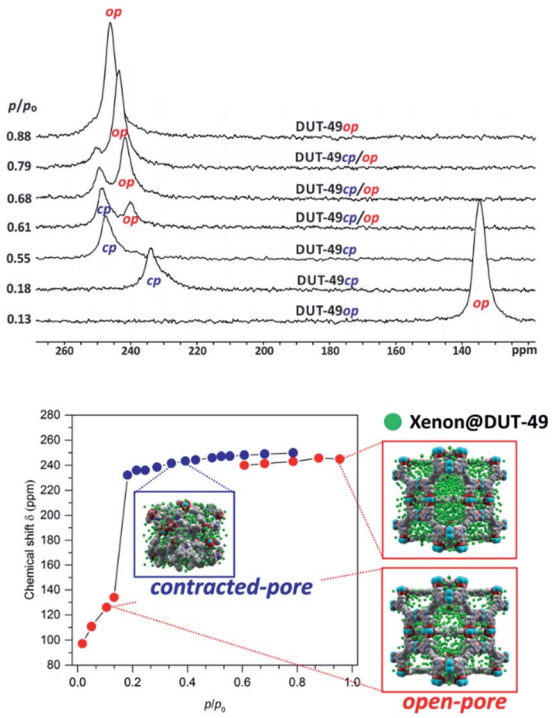

Fig. 5 Top: ^{129}Xe NMR signals of adsorbed xenon on DUT-49 measured at 200 K for various relative pressures during the adsorption experiment (*op*: *open-pore* phase, *cp*: *contracted-pore* phase). Bottom: Chemical shift of adsorbed xenon in DUT-49 at 200 K measured during the adsorption experiment (red symbols denote signals of DUT-49*op*; blue symbols denote those of DUT-49*cp*). Data adapted[63] with permission. Copyright 2017, American Chemical Society.

Conclusions and outlook

Driven by continuous methodical development over decades, ssNMR spectroscopy is nowadays one of the most powerful methods for the determination of the local structure and dynamics of various materials. To date, NMR spectroscopy offers a wide variety of advanced experiments which are increasingly applied to characterize MOFs and their interactions with guest species. On one hand, ssNMR spectroscopy, usually in combination with MAS, allows studying of the local framework structure and adsorption-induced changes of the framework. In the future, these studies will substantially gain from ongoing developments such as the construction of high-field spectrometers beyond 1 GHz ^{1}H resonance frequency, ultrafast MAS probes, and increasing application of novel spin hyperpolarization techniques like DNP.[67] The first DNP-enhanced ssNMR experiments on MOFs have already been reported in the literature.[68–70]

On the other hand, *in situ* NMR approaches with and without MAS allow the characterization of processes like gas adsorption, catalytic reactions, electro-adsorption, and others. *In situ* NMR techniques will find increasing interest in the future. This will in turn stimulate further methodical developments such as novel MAS probes allowing even higher temperatures and pressures. Miniaturized coil design in combination with spin hyperpolarization experiments may allow *in situ* NMR studies in microfluidic applications. Such future *in situ* NMR experiments will be particularly valuable for the characterization of properties and functions of MOFs with

respect to envisioned applications. This will improve the knowledge base and help in designing tailored MOF syntheses in the future.

Conflicts of interest

There are no conflicts to declare.

Acknowledgements

The authors gratefully acknowledge the financial support from the Deutsche Forschungsgemeinschaft within the research unit FOR 2433 "MOF-Switches".

Notes and references

1 H. Furukawa, K. E. Cordova, M. O'Keeffe and O. M. Yaghi, *Science*, 2013, **341**, 974.
2 S. Kitagawa, R. Kitaura and S. Noro, *Angew. Chem., Int. Ed.*, 2004, **43**, 2334.
3 S. Horike, S. Shimomura and S. Kitagawa, *Nat. Chem.*, 2009, **1**, 695.
4 *The Chemistry of Metal-Organic Frameworks*, ed. S. Kaskel, Wiley-VCH, Weinheim, 2016.
5 I. M. Hönicke, I. Senkovska, V. Bon, I. A. Baburin, N. Bönisch, S. Raschke, J. D. Evans and S. Kaskel, *Angew. Chem., Int. Ed.*, 2018, **57**, 13780.
6 C. Serre, F. Millange, C. Thouvenot, M. Noguès, G. Marsolier, D. Louër and G. Férey, *J. Am. Chem. Soc.*, 2002, **124**, 13519.
7 T. Ahnfeldt, D. Gunzelmann, T. Loiseau, D. Hirsemann, J. Senker, G. Férey and N. Stock, *Inorg. Chem.*, 2009, **48**, 3057.
8 G. P. M. Bignami, Z. H. Davis, D. M. Dawson, S. A. Morris, S. E. Russell, D. McKay, R. E. Parke, D. Iuga, R. E. Morris and S. E. Ashbrook, *Chem. Sci.*, 2018, **9**, 850.
9 N. Kavoosi, V. Bon, I. Senkovska, S. Krause, C. Atzori, F. Bonino, J. Pallmann, S. Paasch, E. Brunner and S. Kaskel, *Dalton Trans.*, 2017, **49**, 4685.
10 V. Bon, E. Brunner, A. Pöppl and S. Kaskel, *Adv. Funct. Mater.*, 2020, 1907847.
11 F. Bloch, W. W. Hansen and M. Packard, *Phys. Rev.*, 1946, **69**, 127.
12 E. M. Purcell, H. C. Torrey and R. V. Pound, *Phys. Rev.*, 1946, **69**, 37.
13 G. E. Pake, *J. Chem. Phys.*, 1948, **16**, 327.
14 M. J. Duer, *Solid-State NMR Spectroscopy, Principles and Applications*, Blackwell Science, 2002.
15 K. J. D. MacKenzie and M. E. Smith, *Multinuclear Solid-State NMR of Inorganic Materials*, Pergamon Materials Series, Elsevier Science 2002.
16 A. J. Pell, G. Pintacuda and C. P. Grey, *Prog. Nucl. Magn. Reson. Spectrosc.*, 2019, **111**, 1.
17 E. R. Andrew, A. Bradbury and R. G. Eades, *Nature*, 1958, **182**, 1659.
18 S. Penzel, A. Oss, M.-L. Org, A. Samoson, A. Böckmann, M. Ernst and B. H. Meier, *J. Biomol. NMR*, 2019, **73**, 19.
19 E. Brunner, D. Freude, B. C. Gerstein and H. Pfeifer, *J. Magn. Reson.*, 1990, **90**, 90.
20 U. Sternberg, R. Witter, I. Kuprov, J. M. Lamley, A. Oss, J. R. Lewandowski and A. Samoson, *J. Magn. Reson.*, 2018, **291**, 32.
21 A. Pines, M. G. Gibby and J. S. Waugh, *J. Chem. Phys.*, 1973, **59**, 569.
22 J. Schaefer and E. O. Stejskal, *J. Am. Chem. Soc.*, 1976, **98**, 1031.
23 T. Gullion and J. Schaefer, *J. Magn. Reson.*, 1989, **81**, 196.
24 H. C. Hoffmann, M. Debowski, P. Müller, S. Paasch, I. Senkovska, S. Kaskel and E. Brunner, *Materials*, 2012, **5**, 2537.
25 B. E. G. Lucier, S. Chen and Y. Huang, *Acc. Chem. Res.*, 2018, **51**, 319.
26 Y. T. A. Wong, V. Martins, B. E. G. Lucier and Y. Huang, *Chem.–Eur. J.*, 2019, **25**, 1848.
27 M. de Oliveira Jr, D. Seeburg, J. Weiß, S. Wohlrab, G. Buntkowsky, U. Bentrup and T. Gutmann, *Catal. Sci. Technol.*, 2019, **9**, 6180.
28 V. Stavila, M. E. Foster, J. W. Brown, R. W. Davis, J. Edgington, A. I. Benin, R. A. Zarkesh, R. Parthasarathi, D. W. Hoyt, E. D. Walter, A. Andersen, N. M. Washton, A. S. Lipton and M. D. Allendorf, *Chem. Sci.*, 2019, **10**, 9880.
29 J. Xu, V. V. Terskikh and Y. Huang, *Chem.–Eur. J.*, 2013, **19**, 4432.
30 A. Sutrisno, V. V. Terskikh, Q. Shi, Z. Song, J. Dong, S. Y. Ding, W. Wang, B. R. Provost, T. D. Daff, T. K. Woo and Y. Huang, *Chem.–Eur. J.*, 2012, **18**, 12251.
31 L. A. O'Dell and R. W. Schurko, *Chem. Phys. Lett.*, 2008, **464**, 97.
32 K. Trepte, S. Schwalbe and G. Seifert, *Phys. Chem. Chem. Phys.*, 2015, **17**, 17122.
33 Z. Ke, L. E. Jamieson, D. M. Dawson, S. E. Ashbrook and M. Bühl, *Solid State Nucl. Magn. Reson.*, 2019, **101**, 31.
34 M. Benzaqui, R. S. Pillai, A. Sabetghadam, V. Benoit, P. Normand, J. Marrot, N. Menguy, D. Montero, W. Shepard, A. Tissot, C. Martineau-Corcos, C. Sicard, M. Mihaylov, F. Carn, I. Beurroies, P. L. Llewellyn, G. De Weireld, K. Hadjiivanov, J. Gascon, F. Kapteijn, G. Maurin, N. Steunou and C. Serre, *Chem. Mater.*, 2017, **29**, 10326.
35 G. Mali, M. Mazaj, I. Arčon, D. Hanžel, D. Arčon and Z. Jagličić, *J. Phys. Chem. Lett.*, 2019, **10**, 1464.
36 X. Kong, H. Deng, F. Yan, J. Kim, J. A. Swisher, B. Smit, O. M. Yaghi and J. A. Reimer, *Science*, 2013, **341**, 882.
37 K. Zhu, C. A. O'Keefe, V. N. Vukotic, R. W. Schurko and S. J. Loeb, *Nat. Chem.*, 2015, **7**, 514.
38 M. R. Hansen, R. Graf and H. W. Spiess, *Acc. Chem. Res.*, 2013, **46**, 1996.
39 A. E. Khudozhitkov, D. I. Kolokolov, A. G. Stepanov, V. A. Bolotov and D. N. Dybtsev, *J. Phys. Chem. C*, 2015, **119**, 28038.
40 J. Z. Hu, M. Y. Hu, Z. Zhao, S. Xu, A. Vjunov, H. Shi, D. M. Camaioni, C. H. F. Peden and J. A. Lercher, *Chem. Commun.*, 2015, **51**, 13458.
41 H. Kirchhain, J. Holzinger, A. Mainka, A. Spörhase, S. Venkatachalam, A. Wixforth and L. van Wüllen, *Solid State Nucl. Magn. Reson.*, 2016, **78**, 37.
42 M. Haouas, *Materials*, 2018, **11**, 1416.

43 C. E. Hughes, P. A. Williams and K. D. M. Harris, *Angew. Chem., Int. Ed.*, 2014, **53**, 8939.
44 D. Freude, M. Hunger and H. Pfeifer, *Chem. Phys. Lett.*, 1982, **91**, 307.
45 H. C. Hoffmann, B. Assfour, F. Epperlein, N. Klein, S. Paasch, I. Senkovska, S. Kaskel, G. Seifert and E. Brunner, *J. Am. Chem. Soc.*, 2011, **133**, 8681.
46 M. Rauche, S. Ehrling, S. Krause, I. Senkovska, S. Kaskel and E. Brunner, *Chem. Commun.*, 2019, **55**, 9140.
47 T. Wittmann, C. B. L. Tschense, L. Zappe, C. Koschnick, R. Siegel, R. Stäglich, B. V. Lotsch and J. Senker, *J. Mater. Chem. A*, 2019, **7**, 10379.
48 V. J. Witherspoon, J. Xu and J. A. Reimer, *Chem. Rev.*, 2018, **118**, 10033.
49 X. Kong, E. Scott, W. Ding, J. A. Mason, J. R. Long and J. A. Reimer, *J. Am. Chem. Soc.*, 2012, **134**, 14341.
50 V. Bon, J. Pallmann, E. Eisbein, H. C. Hoffmann, I. Senkovska, I. Schwedler, A. Schneemann, S. Henke, D. Wallacher, R. A. Fischer, G. Seifert, E. Brunner and S. Kaskel, *Microporous Mesoporous Mater.*, 2015, **216**, 64.
51 R. M. Marti, J. Howe, C. R. Morelock, M. S. Conradi, K. Walton, D. S. Sholl and S. E. Hayes, *J. Phys. Chem. C*, 2017, **121**, 25778.
52 Y. Zhang, B. E. G. Lucier and Y. Huang, *Phys. Chem. Chem. Phys.*, 2016, **18**, 8327.
53 Y. Lu, B. E. G. Lucier, Y. Zhang, P. Ren, A. Zheng and Y. Huang, *Phys. Chem. Chem. Phys.*, 2017, **19**, 6130.
54 A. C. Forse, M. I. Gonzalez, R. L. Siegelman, V. J. Witherspoon, S. Jawahery, R. Mercado, P. J. Milner, J. D. Martell, B. Smit, B. Blümich, J. R. Long and J. A. Reimer, *J. Am. Chem. Soc.*, 2018, **140**, 1663.
55 Y. Yan, D. I. Kolokolov, I. da Silva, A. G. Stepanov, A. J. Blake, A. Dailly, P. Manuel, C. C. Tang, S. Yang and M. Schröder, *J. Am. Chem. Soc.*, 2017, **139**, 13349.
56 M. Sin, N. Kavoosi, M. Rauche, J. Pallmann, S. Paasch, I. Senkovska, S. Kaskel and E. Brunner, *Langmuir*, 2019, **35**, 3162.
57 E. M. Forman, B. R. Pimentel, K. J. Ziegler and R. P. Lively, *Microporous Mesoporous Mater.*, 2017, **248**, 158.
58 T. Ito and J. Fraissard, *J. Chem. Phys.*, 1982, **76**, 5225.
59 T. W. Kemnitzer, C. B. L. Tschense, T. Wittmann, E. A. Rössler and J. Senker, *Langmuir*, 2018, **34**, 12538.
60 M.-A. Springuel-Huet, A. Nossov, Z. Adem, F. Guenneau, C. Volkringer, T. Loiseau, G. Férey and A. Gédéon, *J. Am. Chem. Soc.*, 2010, **132**, 11599.
61 R. Giovine, C. Volkringer, M.-A. Springuel-Huet, A. Nossov, F. Blanc, J. Trébosc, T. Loiseau, J.-P. Amoureux, O. Lafon and F. Pourpoint, *J. Phys. Chem. C*, 2017, **121**, 19262.
62 S. Krause, V. Bon, I. Senkovska, U. Stoeck, D. Wallacher, D. M. Többens, S. Zander, R. S. Pillai, G. Maurin, F.-X. Coudert and S. Kaskel, *Nature*, 2016, **532**, 348.
63 J. Schaber, S. Krause, S. Paasch, I. Senkovska, V. Bon, D. M. Többens, D. Wallacher, S. Kaskel and E. Brunner, *J. Phys. Chem. C*, 2017, **121**, 5195.
64 F. Kolbe, S. Krause, V. Bon, I. Senkovska, S. Kaskel and E. Brunner, *Chem. Mater.*, 2019, **31**, 6193.
65 W. Zhang, S. Xu, X. Han and X. Bao, *Chem. Soc. Rev.*, 2012, **41**, 192.
66 F. Blanc, M. Leskes and C. P. Grey, *Acc. Chem. Res.*, 2013, **46**, 1952.
67 A. B. Barnes, G. De Paëpe, P. C. A. van der Wel, K.-N. Hu, C. G. Joo, V. S. Bajaj, M. L. Mak-Jurkauskas, J. R. Sirigiri, J. Herzfeld, R. J. Temkin and R. G. Griffin, *Appl. Magn. Reson.*, 2008, **34**, 237.
68 A. J. Rossini, A. Zagdoun, M. Lelli, J. Canivet, S. Aguado, O. Ouari, P. Tordo, M. Rosay, W. E. Maas, C. Copéret, D. Farrusseng, L. Emsley and A. Lesage, *Angew. Chem., Int. Ed.*, 2012, **51**, 123.
69 F. Pourpoint, A. S. L. Thankamony, C. Volkringer, T. Loiseau, J. Trébosc, F. Aussenac, D. Carnevale, G. Bodenhausen, H. Vezin, O. Lafon and J.-P. Amoureux, *Chem. Commun.*, 2014, **50**, 933.
70 T. Kobayashi, F. A. Perras, T. W. Goh, T. L. Metz, W. Huang and M. Pruski, *J. Phys. Chem. Lett.*, 2016, **7**, 2322.

